VĚDECKÉ SPISY VYSOKÉHO UČENÍ TECHNICKÉHO V BRNĚ
Edice Habilitační a inaugurační spisy, sv. 455
ISSN 1213-418X

Bohuslav Rezek

MICROSCOPIC PROPERTIES OF DIAMOND AND ITS MOLECULAR AND BIOLOGICAL INTERFACES

Brno University of Technology
Faculty of Mechanical Engineering
Institute of Physics AS CR, v. v. i.

RNDr. Bohuslav Rezek, Ph.D.

MICROSCOPIC PROPERTIES OF DIAMOND AND ITS MOLECULAR AND BIOLOGICAL INTERFACES

MIKROSKOPICKÉ VLASTNOSTI DIAMANTU A JEHO MOLEKULÁRNÍCH A BIOLOGICKÝCH ROZHRANÍ

Short version of habilitation thesis

VUTIUM

Brno, 2013

KEYWORDS

diamond, thin films, nanocrystalline materials, DNA, proteins, cells, macromolecules, field-effect transistors, atomic force microscopy, kelvin force microscopy, scanning electron microscopy, electronic properties, surface physics, surface chemistry, in-situ analysis

KLÍČOVÁ SLOVA

diamant, tenké vrstvy, nanokrystalické materiály, DNA, proteiny, buňky, makromolekuly, tranzistory řízené polem, mikroskopie atomárních sil, kelvinovská mikroskopie, rastrovací elektronová mikroskopie, elektronické vlastnosti, fyzika povrchů, chemie povrchů, in-situ analýza

Habilitační práce je uložena v Areálové knihovně FSI VUT v Brně.

ISBN 978-80-214-4763-9
ISSN 1213-418X

TABLE OF CONTENTS

PROFESSIONAL CHARACTERISTICS

Born in 1973 in Prague, Czech Republic, Bohuslav Rezek graduated from Physics at the Faculty of Mathematics and Physics at the Charles University in Prague, continued with PhD. at Academy of Sciences of the Czech Republic (ASCR) in a group of Dr. Jan Kočka on the charge transport in amorphous and microcrystalline silicon with high lateral resolution by the use of scanning probe techniques. During his PhD. he spent several research stays in a group of Prof. Martin Stutzmann at the Walter Schottky Institut, Technische Universität München. There he worked with Dr. Christoph Nebel on development of large grain silicon thin films using interference laser crystallization of amorphous silicon layers and on their investigation by laser beam induced currents with a sub-micrometer lateral resolution, with a special view to optical and electronic properties of grain boundaries. After receiving PhD. degree in 2001, he continued in the group of Prof. Stutzmann as a postdoctoral researcher on the project for diamond devices and sensors where he focused on a study and modification of hydrogen terminated diamond surfaces and their electrolytic interfaces. In 2002 he joined the Nanotechnology Group at the Swiss Federal Institute of Technology, where he was working on a guided assembly of colloidal nanoparticles at solid state surfaces with Prof. Stemmer. Since 2004 he worked at the Diamond Research Center of AIST in Tsukuba, Japan, doing research on surface (bio)-functionalized diamond devices. In 2006 he became research team leader and Purkyně Fellow at the Institute of Physics ASCR in Prague, Czech Republic. Since 2011 he is a head of newly established Laboratory of Functional Nano-interfaces in the same Institute. He is the author or co-author of over 130 scientific articles in international peer-reviewed journals that were cited more than 1600 times and of several patents and patent applications.

His research team is focused on nano-interfaces of semiconductors and organic materials towards opto-electronic and bio-electronic applications. Main interests lie in characterization and modification of material, electronic, and chemical properties by local probe techniques as well as in guided assembly of organic and inorganic microstructures. Physical and chemical parameters are employed to merge these materials and to control their growth, orientation and position. Measurement and correlation of structural, (opto-) electronic and chemical properties and phenomena on a microscopic level plays a fundamental role in this research. Based on the microscopic and macroscopic measurements, physical models of arrangement, properties, and functional mechanisms are constructed. Functionality (such as electrical charge transport and transfer) is characterized with view to target applications in electronics, optics, energy conversion as well as medicine, environment, and security. Indispensable part is an extensive collaboration on national and international level.

More information is available at www.fzu.cz/~rezek

1. Introduction

Understanding and control of interactions between biological environment (tissues, cells, proteins, molecules, electrolytes, etc.) and solid-state surfaces is fundamental for biomedical applications such as bio-sensors, bio-electronics, tissue engineering and implant materials as well as for environmental monitoring, security and other fields. Cells, the cornerstones of living tissue, perceive their surroundings and subsequently modify it by producing extracellular matrix (ECM), which serves as a basis to simplify their adhesion, spreading and differentiation [1]. This process is considerably complex, flexible and it strongly depends on the cell cultivation conditions including properties of the substrate. Surface roughness of the substrate plays an important role [2–5], other factors include in particular porosity [6] and wettability of the substrate. Water wetting properties of the substrate can influence protein conformation [7, 8] as well as the adsorption and viability of cells [9, 10].

Commonly employed substrate materials for *in-vitro* testing are polystyrene and glass. However, diamond as a relatively novel semiconductor material can provide unique combination of excellent semiconducting, mechanical, chemical and biocompatible properties for this purpose [11]. Diamond also meets basic requirements for large-scale industrial applications. Most notably, it can be prepared synthetically either as a bulk material under high-pressure and high-temperature conditions or in the form of thin films by chemical vapor deposition (CVD) from methane and hydrogen on various substrates [12, 13]. In fundamental studies, monocrystalline diamond (MCD) is employed more often than nanocrystalline diamond films because MCD exhibits higher conductivity and better defined structure in comparison to nanocrystalline (or polycrystalline) diamond. On the other hand, NCD films are more likely to be widely applicable as they are inexpensive in comparison to MCD and they can be easily fabricated on almost arbitrary substrates. Nowadays, diamond can be deposited even on large areas (600 cm^2 or more) using linear antennas for spreading microwave plasma during the CVD process [14, 15]. Procedure for selective diamond nucleation enable direct growth of conductive diamond microstructures, which can be operated as transistors or pH sensors [16]. Thus the nanocrystalline diamond can be understood as a class of materials with morphological, chemical, and electronic properties that are adjustable on demand for specific application. However, from electronic and chemical point of view the NCD is a complicated system due to the presence of sp2 carbon phase and grain boundaries. Role of these features still needs to be fully elucidated [17, 18].

Nevertheless, excellent compatibility of diamond with biological materials and environment [9, 10, 19, 20] is of fundamental importance for its application in medicine. The diamond bio-compatibility stems from the fact that diamond is a crystalline form of carbon that is mechanically, chemically and physically very stable. In spite of the general chemical stability, diamond surface can be terminated (functionalized) by various atomic species [21–23] and organic molecules [24–28] which can significantly alter diamond natural properties and thereby lead to new phenomena and applications.

In the most simple case, the molecules can adhere to diamond via physisorption. For instance, fullerene thin films were able to generate stable surface conductive layer (SCL) when deposited on intrinsic diamond [26]. Phenol-formaldehyde and acrylic resins spin-coated on diamond surfaces were also able to stabilize SCL [29]. Pentacene was evaporated on diamond to create novel organic transistors [30]. And as shown in this work, proteins can

be adsorbed for guiding cellular assembly [31–33]. Covalent grafting of molecules to diamond surfaces, i.e. chemisorption, is a favorable option for stable bio-functionalization. Here the hydrogen-terminated diamond surface is an ideal starting point for covalent attachment of organic molecules such as DNA or proteins [24, 25, 27, 34]. Diverse techniques for grafting of various linker molecules or molecules with primary amines were developed and employed during the last decade [34]. But it is not all about biology. Fullerene or polypyrrole grafted to diamond provide interesting energy conversion system for photovoltaic applications [28, 35]. We proposed that the function of such interfaces is enabled exactly by the covalent bond.

Already simple atomic groups terminating the diamond surface can give rise to interesting properties and functions. For example, electrical conductance and electron affinity are both significantly influenced by termination of diamond surface by hydrogen or oxygen atoms [21–23, 36, 37]. The main difference arises from the opposite dipoles of C–H and C–O bonds. Oxygen-terminated diamond is insulating, whereas the hydrogen-terminated surface causes the emergence of two-dimensional hole surface conductance on otherwise insulating diamond. These properties can be exploited for the fabrication of a planar field-effect transistor (FET), gate of which is formed solely by hydrogen surface atoms without any other insulating layer and which is sensitive to pH value in solution [38–40]. On the other hand, the hydrogen-terminated diamond surface is generally less favorable for the adhesion, spreading and viability of cells compared to the oxidized surface [9]. This difference is due to the hydrophilic properties of oxygen-terminated diamond (O-diamond) in contrast to the hydrophobic properties of the hydrogen-terminated diamond (H-diamond). Due to the above features the combination of both hydrogen- and oxygen-terminated diamond surface is promising for bio-electronics [41, 42] as well as for tissue engineering [31, 33].

In this habilitation thesis we present the influence of micro-structured morphology and atomic termination of diamond surfaces on the cell growth and assembly. We investigate the influence of key parameters such as seeding concentration of cells, type of applied cells, and concentration of fetal bovine serum (FBS) in the cultivation medium. We show and explain why adsorption of proteins from the FBS serum is the fundamental factor. Atomic force microscopy (AFM) both in solution and in air is applied to characterize properties of the FBS layers adsorbed on differently terminated diamond substrates. Combination of advanced AFM and Kelvin force microscopy (KFM) or scanning electron microscopy (SEM) is used to recognize physisorption or chemisorption of organic molecules to diamond. The influence of proteins and cells on the electronic properties of diamond is characterized by employing a field-effect transistor based on hydrogen-terminated diamond, gate of which is exposed to an electrolyte solution (SG-FET). Role of grain boundaries in nanocrystalline diamond is resolved and shown not to be detrimental for its function. These results are discussed from the point of view of fundamental physics, biology as well as of the prospects in applications.

2. Fabrication of diamond layers

The growth of thin-film nanocrystalline diamond layers (NCD) was realized on silicon or glass substrates using microwave plasma enhanced chemical vapor deposition (MW-CVD) [12, 13]. The substrates were 10×10 mm^2 large and had surface roughness < 1 nm. Before the deposition, the substrates were ultrasonically cleaned in isopropanol and deionized water

and were subsequently immersed for 40 min into an ultrasonic bath with a colloidal suspension of nanodiamond powder (UDD – ultra-dispersed diamond; NanoAmando, New Metals and Chemicals Corp. Ltd., Kyobashi) with nominal particle size of 5 nm. This process leads to the formation of a 5 to 25 nm thin layer of the nanodiamond powder.

This nucleation procedure was followed by a microwave plasma-enhanced chemical vapor deposition (MW-CVD) of diamond films. The deposition conditions were: temperature of substrates 600–800°C, 1% CH_4 in H_2, microwave power 1.4–2.5 kW, gas pressure 30–50 mbar. Within 1–4 hours the thickness of NCD layers reaches 100–500 nm. In some cases, the nucleation and growth were repeated on the other side of the substrate in order to obtain hermetic encapsulation of the substrate by the NCD layer [31, 33]. The fabrication procedure is schematically shown in Figure 1. This figure also shows photographs of the two set-ups for large-area diamond growth (linear plasma) and for high deposition rate (focused plasma).

Same conditions as for the diamond growth were used for H-termination of the diamond surface where only methane gas was switched off and the process time was reduced to 10 min. Before the H-termination, the NCD layers were chemically cleaned in acids (97.5% H_2SO_4 + 99% KNO_3 powder in the ratio of 4:1) at 200°C for 30 minutes. This process ensures high quality of the H-terminated surface with surface conductance in the order of 10^{-7} S/sq [43].

Surface morphology and chemical quality of the NCD layers were characterized by AFM, SEM and Raman spectroscopy. Surface roughness as evaluated in the tapping AFM regime was typically $15 - 30$ nm rms (1×1 μm^2 area), grain size as measured by SEM was typically $50 - 150$ nm (see Figure 2(a)), in some cases up to 500 nm. The grains exhibit clear facets that evidence their crystalline diamond form. Raman spectroscopy (excitation wavelength 325 nm) confirmed the diamond character of the layers (see Figure 2(b)). With a small alteration of the deposition conditions, grain sizes of even several hundreds of nanometers can be reached.

Polished monocrystalline diamonds (IIa (100), Element Six) were used as reference substrates. Surface modifications were prepared in the same way as on the NCD films.

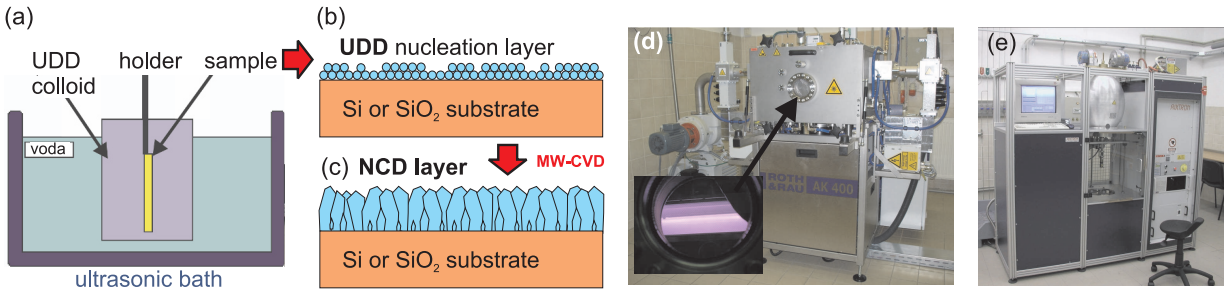

Fig. 1. Schematic depiction of the thin-film diamond fabrication procedure on glass or silicon substrates: (a) nucleation of the substrates carried out in an ultrasonic bath with ultra-dispersed diamond nanoparticles (UDD), (b) the resulting nucleation layer and (c) the nanocrystalline diamond layer after the microwave plasma deposition. The deposition machines for (d) large-area growth of diamond (linear plasma) and (e) high-speed growth (focused plasma).

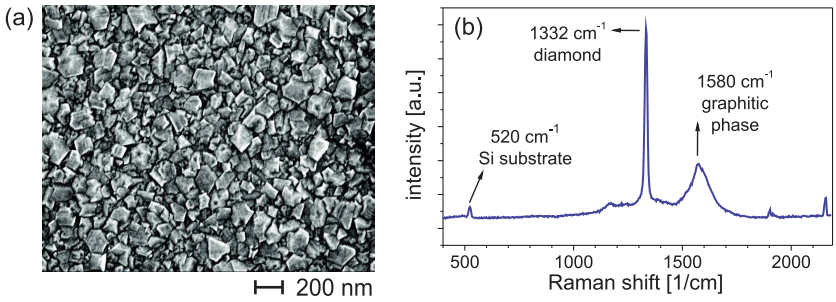

Fig. 2. Basic characteristics of typical NCD layer on Si: (a) SEM morphology and (b) Raman scattering spectrum.

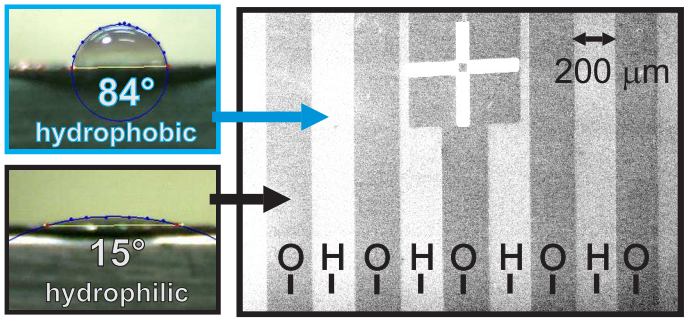

Fig. 3. SEM image of a nanocrystalline diamond layer with 200 µm wide stripes of alternating hydrogen and oxygen termination. Light stripes correspond to the hydrogen surface due to its low electron affinity. The cross in the upper part of the image is made up of a thin layer of gold and serves as a mark for distinguishing the termination of stripes. Typical measurements of water wetting angle on the two types of diamond surfaces (uniformly terminated) are shown along the left side of the SEM image.

3. Assembly of cellular micro-arrays on diamond

3.1 Atomic micro-patterning of diamond surfaces

To characterize influence of diamond surface atoms on the arrangement of cells, we fabricated NCD layers with hydrogen and oxygen surface atoms forming microscopic patterns of 30 to 200 µm width as follows: Positive tone photoresist ma-P1215 (micro resist technology GmbH, Germany) was spin-coated on the NCD surface and micro-patterned by optical lithography. Afterwards, the NCD layers were exposed with a photolithographic mask in high-frequency oxygen plasma (power 300 W, duration 3 minutes). This gives rise to oxidation of the diamond surface and consequently to the formation of hydrophilic patterns. The wetting angle of water on O-diamond was $< 20°$, in contrast to about 80° on H-diamond. Morphology of the surface remains unchanged during this procedure. Figure 3 shows how the microscopic chemical patterns look in SEM. Hydrogen- and oxygen-terminated stripes exhibit different SEM contrast in secondary electrons due to their different electron affinity.

3.2 Preferential cell growth on atomic micro-patterns

Before cell plating, the NCD layers were sterilized using either UV irradiation or 70% ethanol treatment for 10 minutes. This had no effect on diamond surface quality. In most experiments, the cell line of human bone cells (osteoblasts – SAOS-2 cells; DSMZ GmbH) was used. The cells were plated on diamond in the concentrations ranging from 2,500

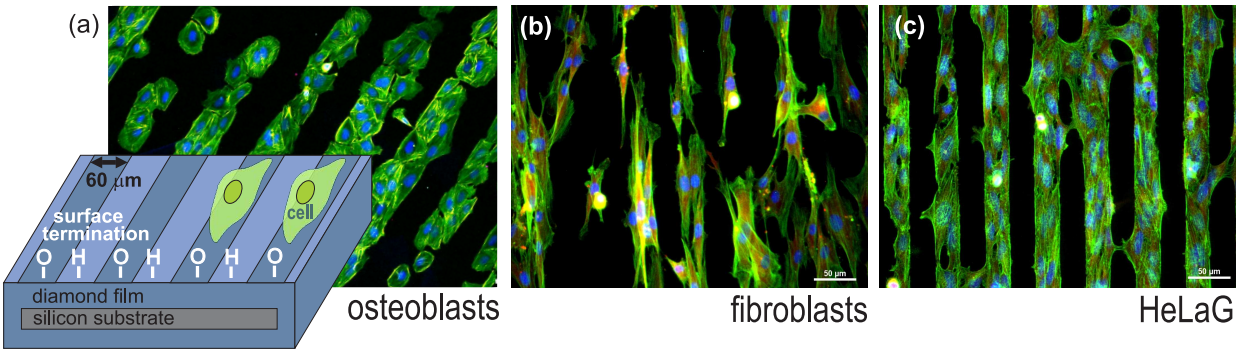

Fig. 4. Microscopic fluorescence image illustrates how (a) osteoblastic cells (SAOS-2), (b) human fibroblastic cells (HPdLF), and (c) cervical carcinoma cells (HeLaG) preferentially self-assemble on oxygen-terminated diamond patterns after a 48h cultivation in medium with FBS supplement.Fluorescence microscopy shows actin filaments in green and cell nuclei in blue. The scheme on the left side illustrates the situation.

(sub-confluent coverage) to 10,000 cells/cm^2 (confluent coverage, when the cells are in direct contact with each other) and immersed in the McCoy's 5A (BioConcept) medium, which contains penicillin (20 U/ml) and streptomycin (20 μg/ml) and different concentrations of FBS (0–15%). Afterwards, the cells were cultivated in an incubator at 37°C, 5% CO_2 for 48h. We used osteoblastic cells because SAOS-2 is a standard cell line, properties of which are stable even during long time spans. In this way we can compare the results of experiments performed at different time as well as in different laboratories and in the literature. Other cell types were also tested for comparison: human periodontal ligament fibroblasts (HPdLF; Lonza) and human cervical carcinoma cells (HeLaG; DSMZ GmbH).

Adhesion and morphology of the cells were characterized by fluorescent staining of actin stress fibers (in green) and cell nuclei (in blue) using the protocol described in [44]. The staining was visualized using the E-400 epifluorescence microscope (Nikon); digital images were acquired with a DS-5M-U1 Color Digital Camera (Nikon).

When the osteoblastic cells were plated and grown on the H-/O-terminated microstructures, they self-assembled preferably on the oxygen-terminated diamond surface. A scheme and fluorescence image shown in Figure 4 give an example of such behavior for the case of 60 µmwide stripes. The cells' preference is independent of the width of the stripes between 30 and 200 µm [33] and of the surface roughness between 20 and 500 nm rms [32]. However, the shape of cells was found to be influenced by the surface roughness [3, 4] and the width of microstructures [31, 33]. Cells grown on narrow O-stripes (30 µm i.e. comparable with the size of the cell) are elongated and form chain-like structures. On the other hand, cells growing on wider stripes (60, 100 a 200 µm – larger than the typical cell size) spread over the whole width of the stripe. The H-/O-diamond boundary forms a sharp interface for cell adhesion.

Other types of cells are also capable of controlled self-assembly on H-/O-diamond stripes. Human fibroblasts and cervical carcinoma cells cultivated on the NCD samples with 30 µm wide stripes exhibit different morphologies compared to osteoblasts. Nevertheless, they also exhibit preference to O-diamond and they form strip-like arrays (see Figure 4b and 4c). Thus the effect of diamond surface atoms on the cell arrangement can be considered a general phenomenon.

Selective growth of cells on H-/O-diamond is influenced by the seeding concentration. At low concentrations (2500 cells/cm^2), the cells grow predominantly on the hydrophilic oxygen-terminated surface where the cells have enough room to spread. On the other hand,

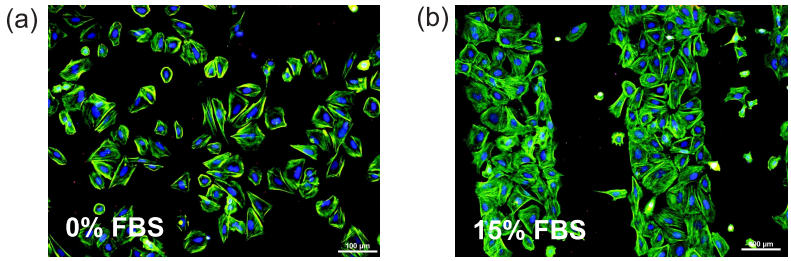

Fig. 5. Fluorescence images of osteoblasts, which were cultivated for 48h on 100-µm-wide H-/O-diamond stripes with different starting concentrations of fetal bovine serum: (a) 0%, (a) 15%. Fluorescence microscopy shows actin filaments in green and cell nuclei in blue. In the 0% case, the cells were plated without the serum, however, the serum was added after 2 hours to allow cells to grow for next 48 h.

cells plated at high seeding concentrations (more than 10000 cells/cm^2) colonize also the hydrophobic hydrogen-terminated surface.

We did not observe significant influence of surface roughness (10–500 nm RMS) or diamond boron doping (100 - 6000 ppm). This shows that the preferential cell arrangement is not due to different conductivity on H- and O-terminated surfaces of intrinsic diamonds and it is solely determined by the action of surface atoms.

The FBS serum is another fundamental factor which has an impact on the preferential growth of cells. Figure 5 evidences the influence of FBS in the cultivation medium on the arrangement of cells on the H-/O-diamond terminated stripes. The range of concentrations between 5% and 15% does not significantly influence the cell adhesion (image for 15% FBS concentration is shown). Nevertheless, the cells plated in the medium without FBS assemble on the surface independently of the surface termination. The cells' preference for a particular type of surface is thus presumably determined by the FBS proteins and not by a direct interaction between diamond surface dipoles and the cells. Therefore, we investigated properties of the FBS layers adsorbed on different types of diamond surfaces.

4. Investigating influence of proteins

4.1 Morphology of protein layers on H/O-diamond

Adsorption, adhesion and conformation of FBS layers on diamond were studied by using AFM. The AFM measurements were carried out in air and in solution both in contact and tapping regimes. Doped silicon cantilevers (Multi75Al, BudgetSensors) with typical spring constant of 3 N/m, resonant frequency 75 kHz in air (30 kHz in solution) and nominal tip radius $<$ 10 nm were used. Polished monocrystalline diamond was used as a substrate to minimize the influence of diamond surface morphology on the layers. Surface terminations were prepared in the same way as in the case of NCD films. The thickness of the protein layer was determined using AFM nanoshaving method, in which a part of the protein layer is removed by means of the AFM tip in contact mode and subsequently the profile of the resulting step in height is measured in oscillating (tapping) mode [8, 27, 45]. This method is described in more detail in Chapter 5.

Being flat and hard, polished monocrystalline diamond represents an ideal substrate for the nanoshaving method. Proteins were adsorbed on the diamond surface from 15% FBS solution (Biowest) in McCoy's 5A medium (BioConcept). Two adsorption procedures were applied:

i) either a drop of the solution was deposited on the substrate by a pipette, the substrate was then kept in a humid chamber for 10 minutes and it was subsequently rinsed with water, or ii) the adsorption was carried out directly in a fluid cell of the AFM microscope for *in-situ* measurement. Both adsorption procedures yielded comparable results. The protein monolayer formed on the diamond surface within several seconds after the application [8].

The AFM nanoshaving experiments showed that thickness of the protein layer adsorbed from the solution is 4 ± 2 nm on O-diamond and 1.5 ± 2 nm on H-diamond [8]. Thus, FBS layers formed on both types of diamond surfaces. Figure 6 presents detailed topography and phase images of the protein layers measured in AFM. Standard deviation values (i.e. RMS – root-mean-square) of the height and phase signals together with the characteristic lateral size of the features (L_x) determined by autocorrelation function are shown below the images. In the case of topography, RMS value corresponds to surface roughness. Roughness of the FBS layer on H-diamond (0.6 nm) is approximately $3\times$ smaller when compared to the O-diamond layer (1.7 nm). Besides, the features on the surface are of different shapes and sizes (12 and 18 nm, respectively). The phase signal exhibits even more pronounced difference. Whereas in the H-diamond case the phase image of the FBS layer consists of dark dots correlating with protrusion in the topography, the O-diamond phase image is characterized by larger bright features, which correlate with round structures in the topography. In AFM experiments in air, such differences in topography and phase channel were not observed [8]. This discrepancy results from the fact that FBS layers are not in their natural environment (solution).

Atomic force spectroscopy detected a characteristic sawtooth profile in the adhesion part (negative force) of the force–distance curve [33]. Typical force curves on H- and O-diamond with adsorbed FBS are shown in Figure 6(e). Amplitude of the sawtooth features is within 500 ± 100 pN. Similar features and force values were detected in force curves on glass-adsorbed proteins where they were attributed to the stretching of the proteins by the AFM tip [46]. The character of the force curves is thus an evidence that the FBS proteins are adsorbed on both types of diamond surfaces.

Based on these AFM measurements, we proposed a model of the proteins conformation when they are adsorbed on diamond surfaces [8]. This model is schematically depicted in Figure 6(f). On hydrophobic surfaces, the denaturation of proteins (i.e. negative conformational change) occurs because their hydrophobic core sticks to the hydrogen-terminated surface. On hydrophilic surfaces, on the other hand, the proteins remain in their natural globular shape. This is why AFM detects a different shape, height and energy dissipation (phase) on the protrusions on the surface. Similar behavior of proteins was observed also on other materials [7], albeit in different range of wetting angles.

4.2 Adhesion and composition of protein layers on diamond

We also considered other factors that may influence the assembly of osteoblastic and other cells on diamonds having H- and O-terminated array patterns. We characterized i) adhesion of proteins and cells to diamond by shaking experiments (1000 rpm), fluorescence, and atomic force microscopy, ii) distribution of FBS proteins by micro-Raman spectroscopy, and iii) influence of pre-adsorbed specific FBS proteins (albumin, fibronectin, vitronectin) on the cell assembly.

We find that presence of FBS on hydrophobic H-diamond reduces adhesion between the osteoblastic cells and this surface. There is 40% lower adhesion of cells on H-terminated diamond with adsorbed FBS compared to this surface without FBS as well as to O-terminated

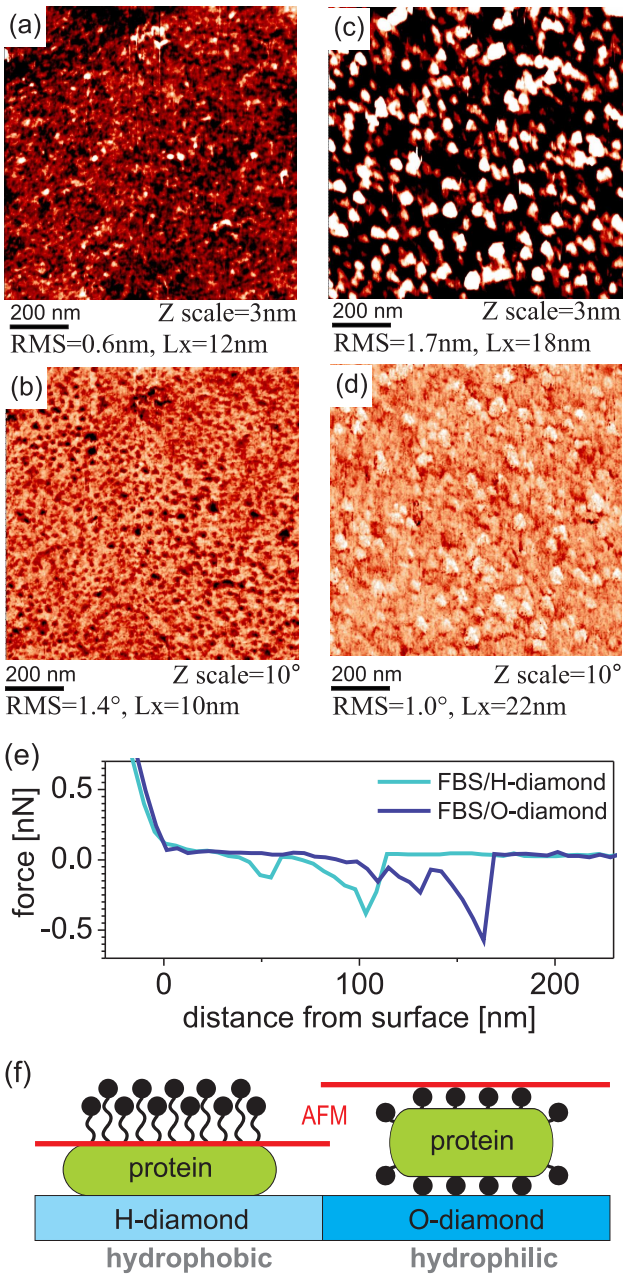

Fig. 6. Atomic force microscopy (AFM) on hydrogen- and oxygen-terminated diamond surfaces with adsorbed FBS layer in FBS/McCoy's medium: topography and phase (a-b) of FBS/H-diamond, (c-d) FBS/O-diamond. Values of standard deviation (RMS) of the height and phase channel and characteristic lateral size of the features (L_x) below the images were determined using the autocorrelation function. (e) Typical atomic force spectroscopy curves for an FBS layer on hydrogen- and oxygen-terminated diamond surface. (f) Model of the conformation of proteins on hydrogen- and oxygen-terminated diamond surface. Hydrophobic core in green, the black spheres represent polar groups surrounding the core in aqueous environment. The red line denotes the height of the protein as detected by AFM in solution.

surfaces. On the other hand, the presence of FBS on hydrophilic O-diamond does not change cell–diamond adhesion strength.

The FBS layer itself also exhibits slightly different adhesion properties as determined by AFM nanoshaving experiments in contact and tapping mode. The adhesion of FBS layers is weaker on H-terminated diamond compared to oxidized diamond surface. This is somewhat surprising as the molecules should "stick" better to H-terminated diamond surface via hydrophobic–hydrophobic interaction. Nevertheless, the adhesion of cells is controlled rather by different protein conformation as the shaking procedure does not remove the FBS layer itself.

By pre-adsorption of specific proteins contained in FBS onto diamond prior to cell plating we find that the cell preference to O-terminated diamond is controlled by fibronectin. Spatially resolved Raman spectroscopy showed, however, only uniform coverage of H/O-diamond by BSA which is the dominant protein in FBS. This was obtained on more than 50 nm thick layers though because few nm thin protein layers, which are typically formed during the cell plating, were not detectable by Raman. Hence Fn may still be present in the adsorbed FBS layers and further experiments by AFM and FTIR are in progress to elucidate its presence, spatial distribution, and biological activity (conformation) on H- and O-terminated diamond. Another question is the protein binding to the surface

5. Recognizing molecular physisorption and chemisorption

As described in the introduction, proteins and other organic molecules can bind to diamond surfaces by two general mechanisms: physisorption and chemisorption. Specific type of binding can profoundly influence electronic exchange at the interface, the interface stability as well as its activity in applications. However, recognition and discrimination between physisorption and chemisorption is not easy in such all-carbon system. Covalent binding of functional organic molecules (DNA, polypyrrole, proteins, enzymes, etc.) to diamond often occurs via just one more carbon-carbon bond in a linker molecule or the functional molecule itself. XPS thus cannot provide unambiguous information about the bond formation. Therefore, we have developed and employed novel methodologies based on scanning probe methods [27, 47–50]. In the following we demonstrate the use of this methodology on several examples: DNA–diamond interface, protein–diamond interface, and PPy–diamond heterojunction.

5.1 AFM nanoshaving and KFM on DNA–diamond interface

The recognition of physisorption and chemisorption proceeds in several steps. At first, mechanical properties of molecular layers are characterized by variation of loading force on the AFM tip in contact-mode AFM mode (CM-AFM). The experiment is schematically shown in Figure 7. When the force is high enough the tip starts to scrape off the molecular layer from the surface. This regime is denoted as AFM nanoshaving. Typical forces are in the range of 1–500 nN, size of probed area is 1–10 μm, and scan rate 1–10 μm/s. The area scanned in CM-AFM is then characterized by non-contact or semi-contact AFM mode (often so-called tapping, TM-AFM). In the TM-AFM the forces are very low, in the order of 0.1 nN or less, so that integrity of the molecular layer is preserved. Yet note that sometimes even tapping mode (TM) nanoshaving can lead to removal of weakly bound molecules such as proteins [47]. We

can consider this regime as an ultra-low force nanoshaving. The TM nanoshaving thus enables us to visualize even slight differences in molecular adhesion.

The mechanism of a molecule removal provides the first hint on the molecular layer arrangement. If the the layer is removed completely straight away, it is most likely composed of individual molecular chains attached to the surface. If only certain thickness of the layer is removed, it indicates a multi-layer structure [51]. In some instances though, it may indicate also compression of the layer [27]. If the layer is not removed but rather disturbed like a layer of snow by a stick, it indicates non-covalent adhesion to the surface [27, 47]. This different behavior is illustrated in Figure 8 on the case of DNA–diamond interface, which was prepared by photochemical grafting [24, 45]. The force of $\geq$ 45 nN is required to remove DNA molecules from initially H–terminated diamond. On initially oxidized samples the DNA layers are mechanically very unstable, the threshold removal force is only 6 nN. The DNA removal on both types of substrates was confirmed by fluorescence microscopy of labelled DNA strands. The area where the DNA was removed by CM-AFM exhibits no fluorescence intensity (see Figure 8(c)).

Further information is provided by the threshold force necessary for the removal of molecules. The threshold force is found by gradually increasing the force on the tip during

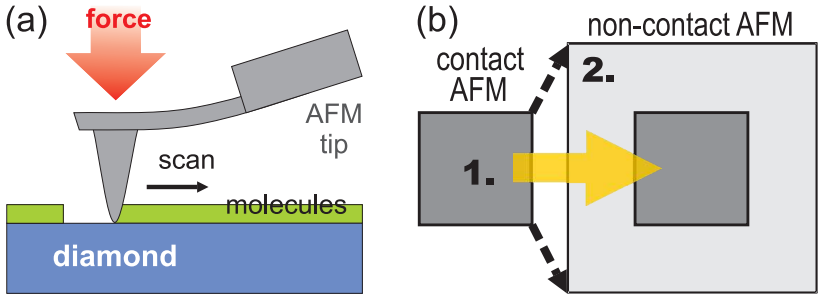

Fig. 7. (a) Scheme of AFM nanoshaving experiment: loading force is applied on the AFM tip so that it penetrates the layer of molecules on diamond and scrapes it off during lateral scanning. (b) Procedure for evaluation of the AFM nanoshaving experiment by non-contact or semi-contact (tapping) mode AFM.

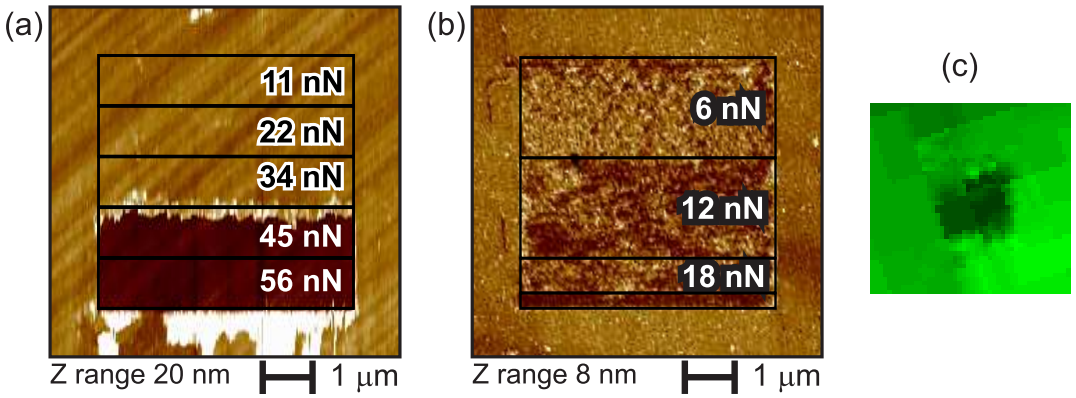

Fig. 8. Non-contact mode AFM images demonstrating removal of DNA using contact mode AFM on photochemically processed diamonds which were initially (a) H–terminated and (b) oxidized. (c) Fluorescence microscopy image of the area where DNA was removed by contact mode AFM.

CM-AFM scanning. The characteristic value for covalent bond is 40–80 nN [51]. Non-covalent bond leads to typical forces < 10 nN [27].

However, there are several problems with determining and using force thresholds for discrimination between physisorption and chemisorption of molecules to diamond and other surfaces. First of all, the AFM tips must be sharp enough. Blunt tips will obviously lead to significantly (orders of magnitude) larger forces needed for scraping off the molecules. This is because for such tip it is more difficult to penetrate the molecular layer. Similar situation occurs when the molecular layer is cross-linked, e.g. a polymer network is formed instead of individual chains. One can actually use the large force threshold (> 100 nN) as an indication of such cross-linked condition if the tip is sharp (i.e. in out of the box condition with typically 10–20 nm radius).

Due to these problems the AFM nanoshaving may not be fully conclusive for recognition of molecular grafting. Here KFM and diamond as a substrate become helpful. KFM proved to be sensitive tool for chemical and electrical characterization of numerous materials, nanostructures, and junctions [52]. This method combines AFM with the a Kelvin probe technique. The technique is based on vibrating parallel plate capacitor which in this case is formed by a sample and AFM cantilever. Due to the difference in the work function of the two materials a contact potential difference (CPD) arises. When a.c. voltage is applied to the AFM cantilever, the CPD leads to alternating electrostatic force exerted on the cantilever and consequently to electrostatically driven cantilever vibrations. The CPD is then compensated by external d.c. voltage applied to one of the plates (tip or sample) so that these vibrations are cancelled. Thereby, an absolute value of CPD is obtained at the measured spot. The KFM thus enables quantitative mapping of electrical potential with high spatial resolution down to nanometer and atomic scale [53]. Different materials, surface chemical groups, localized charges, depletions regions, photo-voltages and much more can be resolved microscopically by using the KFM measurements [22, 35, 52].

Because of well defined electronic and chemical properties of diamond surface, the change of surface potential measured by KFM in nanoshaved regions is a clear indication of a change of diamond surface atoms [22, 27]. This methodology is illustrated in Figure 9 on the case of DNA–diamond interface, more specifically on DNA linker molecules. While the initial H-terminated diamond surface exhibits same KFM potential as the gold layer (within 50 mV) [22], the shift of 400 mV is observed after grafting and removal of the molecules.

5.2 Protein–diamond interface

We applied the above methodology also for the protein–diamond interface. Figure 10 shows AFM surface morphologies of the nanoshaved FBS protein layers on oxidized diamond and H-terminated diamond. The forces of 5 nN and 10 nN as well as mechanism of the removal ("stick in snow") indicated non-covalent binding of the FBS proteins to the diamond surface [48]. Although no specific procedure was applied to graft the proteins to diamond, it could occur also non-intentionally via interaction of amine groups in the proteins with H-terminated diamond surface as reported recently [54].

The difference between 5 nN and 10 nN on H-terminated and oxidized diamond is reproducible and significant. It is not due to a change in the AFM tip sharpness because the larger force was determined before the smaller force. This subtle yet distinct difference was

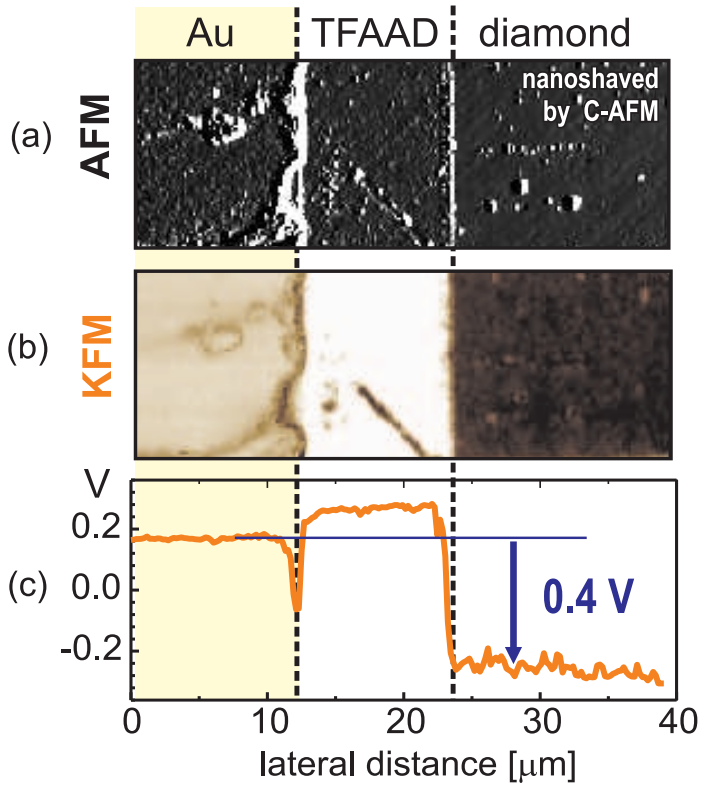

Fig. 9. (a) Non-contact AFM surface morphology in air across gold contact, DNA linker molecular layer, and diamond surface region where the linker layer was removed by contact mode AFM (threshold force 45 nN). (b) KFM image and (c) KFM profile of surface potential across the same regions.

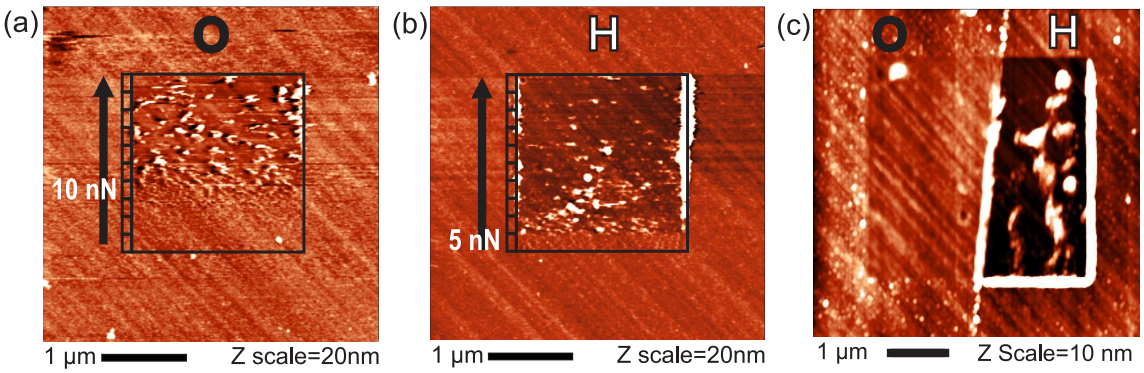

Fig. 10. Non-contact AFM surface morphologies in air across the region where FBS protein layer was removed by contact mode AFM: (a) oxidized diamond (threshold force 10 nN), (b) H-terminated diamond (threshold force 5 nN). The arrow shows slow-scan axis direction of the AFM nanoshawing. (c) Non-contact AFM surface morphology showing results of tapping mode nanoshaving of FBS protein layer at the boundary of H-terminated and oxidized diamond.

confirmed also by TM nanoshaving across the boundary of H-terminated and oxidized diamond as shown in Figure 10(c). The protein layer was removed by TM on H-terminated part of surface while it persisted on oxidized part [47].

5.3 PPy–diamond heterojunction

For creating another type of organic–inorganic junction with potential bio-sensor as well as opto-electronic functions, we electrochemically synthesized polypyrrole (PPy) on diamond from pyrrole (0.24 M) and NaCl (0.1 M) aqueous solution by the application of a constant current (current density typically -0.3 mA/cm^2). In the first instance we employed a hydrogen-terminated intrinsic monocrystalline diamond (synthetic IIa (100) CVD diamond) with conductive surface as a working electrode [55]. PPy was electrochemically synthesized on the channel as shown in Figure 11(a).

Then we applied contact-mode AFM with increasing contact force. At certain threshold contact force, the sharp tip starts to penetrate and remove the organic film. This transition is evidenced in Figure 11(b). The threshold force deduced in this manner was about 40 nN. This value is comparable to the values observed on a system consisting of diamond with covalently grafted DNA molecules [45, 51]. This indicates that in this case the PPy molecules form linear chains with covalent bonds to H-terminated diamond.

Surface potential measured by KFM on the place where the PPy film was deposited and removed (Figure 11(c)) is significantly lower (by about 0.1 V) than the potential on pristine H-terminated diamond surface. This change is similar to reports on DNA–diamond interfaces [27] and supports the assertion of PPy molecules being linked to diamond surface covalently while removing the H termination. We also observed that the surface conductivity disappeared after the synthesis and the removal of the PPy molecules from diamond surface, which is another evidence of the missing H termination.

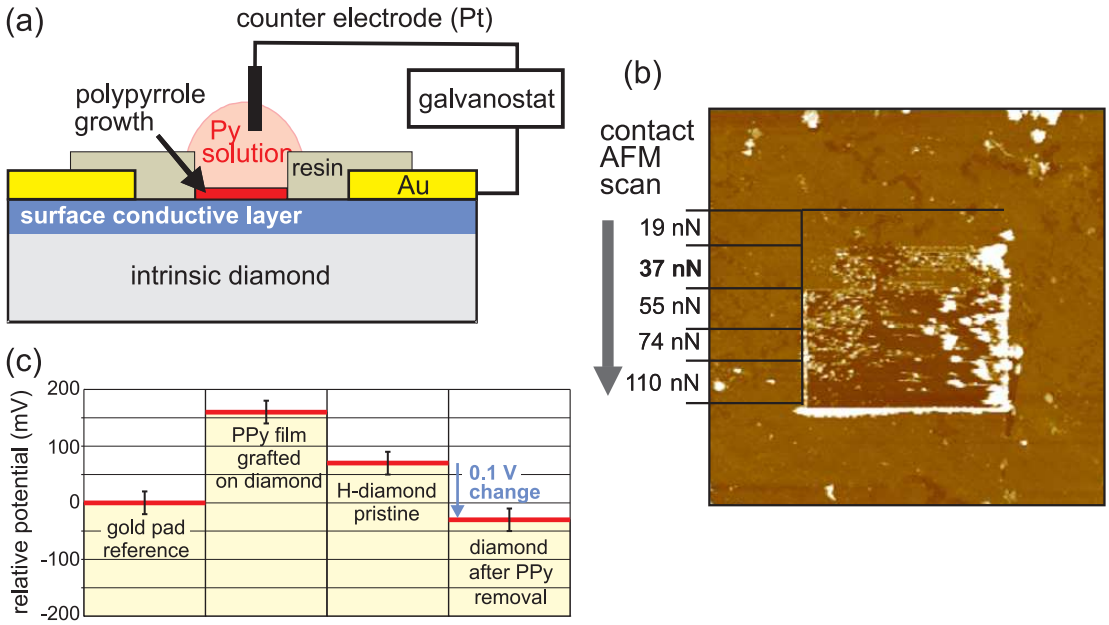

Fig. 11. (a)Schematic cross-sectional drawing of experimental setup for electrochemical synthesis of PPy on the diamond device structure. (b) Scratching of the PPy film by AFM tip with increasing contact force shows that forces reaching 40 nN are strong enough to remove PPy molecules from the diamond substrate. (c) Average surface potential obtained by KFM on PPy-diamond, H-diamond, and diamond after PPy removal. The potential values are referenced to the grounded Au contact pad.

Covalent bonding between PPy and diamond was confirmed also theoretically. Calculated interaction energy of about 6 eV per bond pointed to a covalent character of the bonds formed as single- or multi-bond contacts between PPy and diamond [56].

Based on the above experimental and theoretical results, we proposed a model for the electrochemical synthesis of PPy on diamond where the hydrogen atoms are removed and PPy molecules establish covalent bonds with carbon atoms of diamond [49].

5.4 AFM nanoshaving and SEM

To study possible specificity of hydrogen-pyrrole reaction and to compare properties of PPy on hydrogen- and oxygen-terminated diamond, in particular formation of covalent bond, we used boron-doped diamonds (BDD). As undoped oxygen-terminated diamond is highly electrically resistive, low doping of diamond by boron (amount of charge carriers at room temperature 10^{14} cm^{-3}) was used to achieve reasonable conductivity of oxidized diamond (resistance 2.4 MΩ) yet to minimize influence of boron in the study. We confirmed that the low boron doping makes BDD conductive enough for electrochemical growth of PPy on both hydrogen- and oxygen-terminated surfaces [50].

The use of KFM for molecular recognition can be sometimes challenging, time consuming, it needs experience to exclude measurement artifacts, and it may not always be available in the laboratory. Therefore, we extended our methodology for the use of SEM, as the change of diamond surface atoms can lead also to a change in the intensity of secondary electrons [22, 33, 50]. AFM contact mode nanoshaving was applied to remove PPy layer as well as a contamination layer from diamond substrate prior to SEM measurements. This was necessary because even pristine diamond surface is typically contaminated by adsorbed hydrocarbon species. The adsorbate layer has thickness below 1 nm, however, it clearly influences both SEM and KFM results [57, 58].

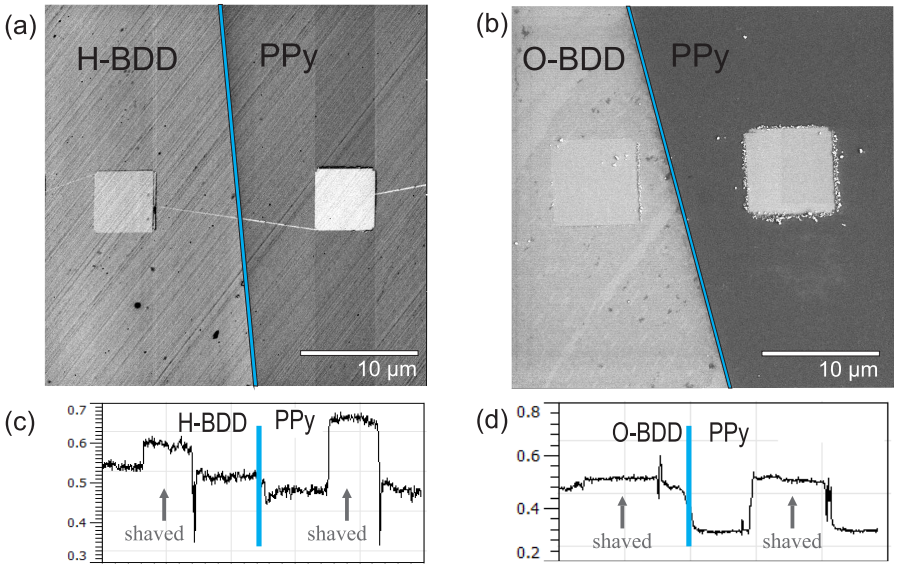

Fig. 12. (a) SEM image obtained at the border between electrochemically deposited thin (5 nm) PPy layer and pristine BDD surface in the case of (a) oxidized BDD or (b) H-terminated BDD. The squares correspond to the nanoshaved regions. (c-d) Corresponding SEM intensity profiles across the nanoshaved squares. The blue lines denote diamond/PPy border in the images and the profiles.

Figure 12 shows that SEM detected change of secondary electron emission on H-BDD surface after PPy growth and removal, from which covalent grafting of PPy to H-BDD via electrochemical synthesis was deduced based on the model of energetic bands and electron affinity. It is well correlated with the change of work function as observed by KFM. It is also in a good agreement with previously observed covalent grafting of PPy to H-terminated intrinsic diamond. On the other hand, no changes in SEM contrast were observed on O-BDD. Therefore, we concluded that no chemical bond between PPy and diamond was formed in this case. We obtained similar SEM data also on highly boron-doped diamond substrates. Thus the electrochemical growth of PPy can be achieved on both H- and O-BDD but the diamond surface atoms (H, O) determine the type of PPy-diamond bonding. Similarly AFM/SEM combination can be applied to other molecules and various adsorption and grafting processes on diamond.

6. Electronic effects at diamond-protein-cell interface

6.1 Solution-gated diamond field-effect transistors

For characterizing influence of the adsorbed molecules and cells on the electronic properties of diamond we created solution-gated field-effect transistor (SGFET) structures to serve both as a practical tool and potential sensor device [41, 59, 60]. Hydrogen-terminated stripes surrounded by oxygen-terminated areas were utilized as conductive channels of the *p*-type diamond SG-FETs [39]. The top-view and cross-sectional diagrams of the SG-FET transistor are shown in Figures 13(a) and 13(b), respectively. Electrical contacts were prepared by thermal evaporation of thin metal layers (10 nm Ti and 50 nm Au) over a photolitographic mask and the subsequent application of the lift-off technique. The transistor was insulated from the electrolyte using a layer of photoresist (1.5 μm thick ma-P1315 or 5 μm thick SU8-3050). Openings of 60×60 μm^2 were introduced in this insulating layer to define the active gate area of the transistor. These openings exposed the surface of the 20 μm wide conductive channel and partly also the surrounding oxidized surface (about 20 μm from each side). The transistor gate was generated by immersion of the active gate area into the solution (electrolyte) which is in contact with an Ag/AgCl reference electrode. The SG-FET gate is insulated merely by hydrogen surface atoms without any other insulating layers. Thus proteins and cells interact directly with the surface of diamond.

Output and transfer SG-FET transistor characteristics were measured using two Keithley K327 source-measure units connected according to Figure 13(a). The characteristics were acquired in the following solutions: (a) McCoy's 5A medium, (b) McCoy's 5A medium with 15% FBS and (c) McCoy's 5A medium with Britton-Robinson buffer at pH = 7. In order to ensure that the acquired characteristics represent stable data, all the measurements were repeated three times.

Output characteristics in Figure 13(c) confirm that nanocrystalline-based transistors are fully functional in solution and their behavior under gate voltage is in accordance with expected *p*-type channel function (positive gate voltage closes the channel). This functionality was reached even in NCD layers as thin as 100 nm with the average grain size of (80 ± 50) nm [18]. The influence of the protein adsorption and subsequent growth of cells on the electronic properties of diamond can be easily recognized in Figure 13(c) which displays transfer characteristics of a pristine diamond transistor (blue), the same transistor after the adsorption

of FBS (red) and after SAOS-2 cell cultivation (green). All characteristics were acquired in the McCoy's 5A medium, source-drain voltage was kept constant during all the measurements (-0.6 V; this setting corresponds to the amplification regime of the transistor). A slight hysteresis effect was observed in all transfer characteristics due to diamond–electrolyte interface [16]. Current flowing through the SG-FET transistor decreased after the application of FBS and the transfer characteristics shifted approximately by -45 mV for $I_{ds} = -0.6$ nA. Another shift by -78 mV was observed after the cultivation of cells, giving rise to the overall shift of about -123 mV. Apart from the shift, the steepness of the slope (transconductance) defined as $g_m = \delta I_{ds}/\delta Ug$ decreased from 9.5 to 8.3 nS at $I_{ds} = -0.6$ nA.

UV sterilization, an important step prior to cell culture process, did not cause another shift after FBS adsorption. Similar characteristics after the sterilization indicate that the protein layer and SG-FET properties do not change during sterilization [61]. Also rinsing the sample with the McCoy's medium had only little impact on the characteristics. Transistor gate (leakage) currents were in the order of 10 pA. Typically, FBS adsorption on the surface reduced the gate currents as FBS forms additional layer on the diamond surface. Yet in some cases the currents slightly increased (to about 40 pA) as a result of the protein adsorption [41].

6.2 Role of grain boundaries in diamond SG-FET

From electronic point of view NCD is a complicated system due to the presence of sp2 carbon phase and grain boundaries and role of these features for biosensors and bioelectronics is not yet understood. Therefore, we employed NCD films of different grain sizes to characterize and discuss influence of grain boundaries and sp2 phase on the SGFET function [18]. We

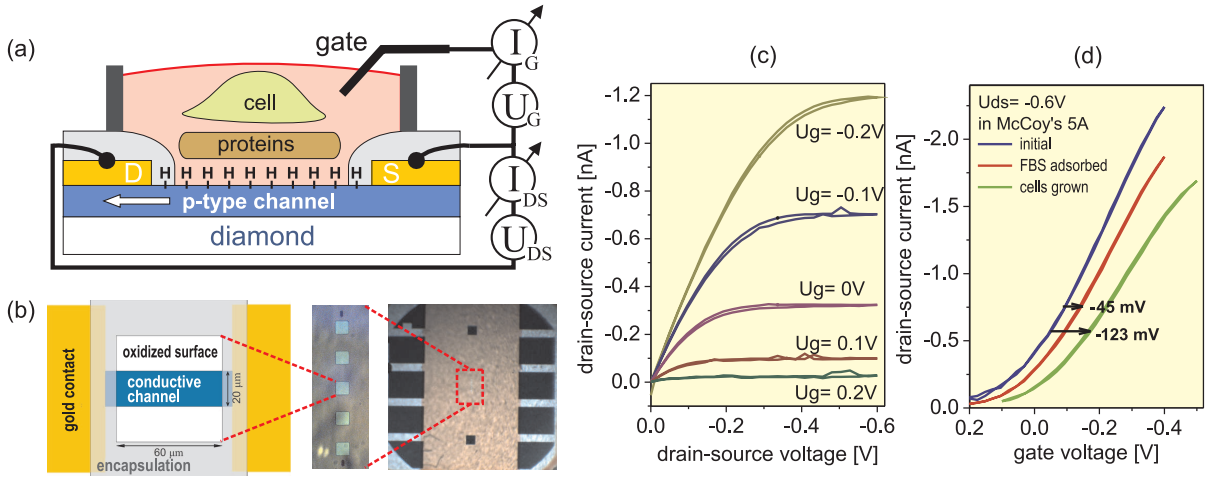

Fig. 13. (a) Diagram of a solution-gate field-effect transistor (SG-FET) based on the surface conductivity of hydrogen-terminated diamond. The insulation of the SG-FET gate is ensured merely by the hydrogen termination of the diamond channel surface. (b) Top-view: hydrogen-terminated conductive microscopic channel is surrounded by insulating oxygen-terminated areas and the active area is determined by the hole in the insulating layer. A chip contains several such areas, as is demonstrated in the optical image of the whole chip (10×10 mm^2 with 5 transistors) on the right. (c) Output characteristics of SG-FET transistor from nanocrystalline diamond in McCoy's 5A solution with gate potential between -0.2 and 0.2 V. (d) Transfer characteristics of a transistor in McCoy's 5A solution at the beginning of the experiment (blue), after the adsorption of proteins from FBS (red) and after 48h cell cultivation (green)

showed that intrinsic nanocrystalline diamond films with average grain sizes down to 80 nm, thickness down to 100 nm, and p-type surface conductivity generated by H-terminated surface are fully operational as SGFETs on glass substrates. We demonstrated that inherent hysteresis of SGFET transfer characteristics, their reaction time to changes of gate potential, their negative shift after protein adsorption and cell culturing process, low gate leakage currents and no influence of UV sterilization or rinsing are all independent of the NCD grain size. By Hall effect experiments we confirmed that the grain boundaries in H-terminated NCD reduce the charge carrier mobility by three orders of magnitude, yet the charge carrier concentration in the surface conductive layer is comparable to monocrystalline diamond. Thus we proposed a microscopic model where the function of NCD SGFET is determined by the H-terminated surface of diamond nanocrystals and its interaction with proteins, not by grain boundaries or sp2 phase between grains.

7. Discussion of diamond-protein-cell interactions

Interaction of cells with as-grown and nanostructured diamond surfaces indicates that the diamond surface morphology can be tailored in a controlled way with respect to bio-technological and bio-medical requirements. It also demonstrates that quite wide range of diamond surface morphologies is acceptable for the cell growth. This is in agreement with other experiments on diamond films where hierarchically modified substrate roughness was employed [4].

In the case of nanostructured diamond surfaces [5], amount of vinculin detected by fluorescence microscopy can be used an indication of the cell motility on the substrate because vinculin generally serves as a stabilizing protein in the focal adhesion [62]. Increased expression of vinculin on diamond nano-cones promotes the cell adhesion and reduces the cell motility. On diamond nano-rods, solitary cells have more chance to move and search the entire space, whereas cells in confluent layer could be easily peeled off.

In the case of hydrogen- and oxygen-terminated microstructures, the cells preferably self-assemble on the oxygen-terminated regions. The growth of cells over the hydrogen-terminated areas, mostly at high cell concentrations, is presumably enabled by their link to the O-diamond layers because individual cells exhibit poor adhesion to H-diamond and reduced metabolic activity [9, 31]. Such cells most likely communicate, exchange growth factors and various stimuli and gradually form the extracellular matrix (ECM). In this way, they modify the surface with proteins and proteoglycans to overcome the unfavorable properties of the substrate. This process enabled us to grow the cell also over the less favorable, but electrically active H-diamond SG-FET channels.

Figure 5 clearly demonstrates that the FBS proteins are the factor whose influence determines the cell adhesion on the diamond layer. As the protein adsorption proceeds much more rapidly than the transport of cells to the surface, the interaction of the cell with the diamond substrate results from the nature of this adsorbed layer. AFM measurements show that proteins adsorb on both types of surfaces, which agrees well with experiments carried out on other materials, where albumin adsorbs both on hydrophilic and on hydrophobic surfaces [7]. The selectivity of the cell growth is thus not determined by FBS adsorbing solely on one type of surface. Other factors, such as denaturation of proteins on hydrophobic surfaces, need

to be taken into account in order to successfully explain the selective adsorption. Detailed study of surface morphology using the AFM method clearly confirms that differences in surface roughness, morphology as well as phase contrast between the protein layers on H- and O-diamond exist. On H-diamond the FBS proteins probably adopt the conformation where their epitopes (e.g. adhesion mediated RGD sequences of peptides) are hidden and thus do not provide optimal conditions for cell adhesion. A similar difference in protein morphology was observed on polystyrene substrates [7]. This is why the wetting properties of a surface seem to be the most influential factor for the growth of cells, whereas other specific properties of diamond layers do not play such an important role. As we have shown, this phenomenon is general and valid also for other types of cells.

The above described preference of the cells for oxygen-terminated surface on H/O-patterned diamond is detectable as early as during the first two hours of adsorption in the 15% FBS supplemented medium [33]. However, the pattern is not yet as sharp as after 48h because the cells did not have enough time to spread on the surface. On the other hand, in a control experiment without FBS the patterned self-assembly was not observed. This implies that even the initial stage of the assembly is strongly influenced by the FBS proteins. In this stage, cells move and actively explore their surrounding environment.

Other factors that can influence the selective cell growth include a different adhesion of cells and proteins to hydrogen- and oxygen-terminated surface. Also a differences in composition of the protein layer on each type of surface can play role. Adhesion of cells to the hydrogen-terminated diamond lowered by as much as 40% was observed in the presence of FBS in comparison to oxygen-terminated diamond [48]. Furthermore, fibronectin, one of the FBS components, was found to have the crucial influence on the selective growth of cells [48]. Detailed composition of the FBS layer on diamond, however, has not yet been successfully identified.

In the medium without FBS, the cells cannot detect any protein layer and thus they are in direct contact with the NCD substrate. After a short time (2 hours), the cells are not yet fully spread, but their contacts (focal complexes) with the substrate are already detectable [33]. In general, the adhesion mechanism is not yet understood. After further cultivation time (48 hours) in the medium where FBS was added, the cells assume normal shapes and growth takes place properly at the spots where the cells initially attached (see Figure 5(a)), most likely because they had enough time to produce their own extracellular matrix and adapt the surface underneath them. The hydrogen- or oxygen-termination of diamond (without the initial activity of the FBS proteins) is, therefore, not the sole factor determining the cells selectivity by itself.

From the point of view of electronic properties of the diamond-protein-cell system, SG-FET diamond transistor exhibits a shift in transfer characteristics towards negative gate voltages after the FBS proteins adsorbed on the channel surface and subsequently the cells were cultivated on top of them. This is a clear sign of reduced transistor conductivity. This effect cannot be fully explained solely by the electrostatic field effect. The major FBS proteins (albumin, fibronectin, vitronectin) as well as cell membranes are negatively charged under physiological pH. Thus, their presence near the gate of a *p*-type transistor should increase the source–drain current through the transistor. This is not the case though.

We proposed another model to explain the electronic effects at the interface between the channel of the diamond SG-FET and the cell medium containing proteins and cells [41]. Figure

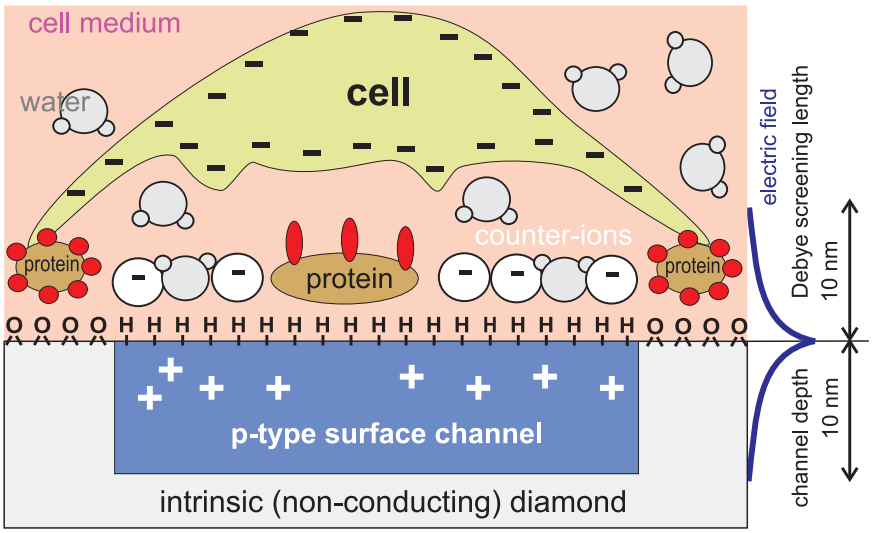

Fig. 14. Schematic sketch of the interface between the surface-conductive SG-FET channel and cell medium containing proteins and cells. The electric field and its reach from the interface is depicted on the right.

14 depicts a schematic concept of this model. The model considers that osteoblastic cells attach to the surface only in a limited number of spots (the so-called focal adhesion), which cannot cover the whole gate area, and the remaining cells are not in direct contact with the substrate surface [4]. Moreover, cells on H-diamond do not tend to spread and adhere but they rather form bridges to O-diamond if it is in a close proximity [31]. The adhesion of osteoblasts is then mediated by proteins, i.e. another FBS protein layer exists between the cell and the diamond surface. This is why the most part of a cell membrane is presumably further than the Debye length in the medium, which amounts to < 10 nm due to the presence of salts and other ionic compounds in the cultivation medium.

As already mentioned, proteins become denatured on a hydrophobic surface and their hydrophobic core sticks to the surface. Consequently, they can modify the initial equilibrium of the conductive layer, which is a result of the equilibrium of chemical potentials of the diamond and the solution [23, 63]. A negative shift occurs as a result of the change of the material properties of diamond (i.e. its conductivity), which is in accordance with the lowered steepness of the slope of the transfer curve (transconductance). Sometimes observed increase in the SG-FET gate currents indicates that proteins can lower the electronic barrier of the diamond-electrolyte system resulting from the surface C–H dipoles [41] and can therefore facilitate the charge transfer across the interface. The primary FBS monolayer persists on the surface [8, 47, 48] and cannot be easily removed by common rinsing methods, even when detergents and enzymes are employed. This explains the stability of the shift in the SG-FET transfer characteristics.

A negative shift of transfer characteristics was observed also after the cultivation of cells on the device. This shift cannot be ascribed to the cells themselves, because it persists even after the cells are removed [61]. Possible reason of this potential shift could be a change in the adsorbed layer of proteins, which remains on the diamond surface even after rinsing [8, 47]. Cells can actively participate at such changes because osteoblasts continually modify their surrounding environment and subsequently produce their own ECM. However, AFM measurements indicated that the morphology of protein layers did not change after 48h

cultivation. Thus the shift after the long-term cultivation is most likely related with the diamond itself. This effect needs further study. Further research should also answer the question concerning the composition of the layers adsorbed on diamond and the possibility of direct electrical detection of the function of cells using the interface with diamond, as has already been suggested for neurons [42].

8. Conclusions

In conclusion, we have characterized some of the fundamental properties and discussed prospective application of diamond for molecular and biological interfaces. We demonstrated that the combination of oxygen- and hydrogen-terminated surface patterns enables controlled self-assembly of human cells into microstructures. Cells preferably adhere to oxygen-terminated areas. This effect is general and occurs for various types of cells. The best selectivity is achieved for low cell seeding concentrations (2500 cells cm^2) regardless of the geometry of the surface and usual range of FBS concentrations (5 to 15%). Higher seeding concentrations enable the cells to colonize even less suitable hydrogen-terminated surface, which is electrically conductive and thus it can be utilized in electronic components. Cells seeded in the medium without FBS colonize the surface independently of the micro-patterns. Thus the cell preference stems from the properties of the proteins on H- and O-diamond and it is not a direct consequence of the cell interaction with diamond surface dipoles.

Atomic force microscopy revealed existence of a thin film (2–4 nm) of proteins on both types of surfaces. However, the proteins adopt different conformations on different surface terminations. We developed and employed a unique methodology based on AFM, KFM and SEM measurements for recognizing physisorption or chemisorption of proteins and other organic molecules on diamond. Thereby we for instance confirmed non-covalent binding of the FBS proteins to the diamond with both hydrogen-terminated and oxidized surface. We also discussed limitations of this methodology. Based on these measurements, we proposed a model where proteins arrange on diamond according to wettability of its surface. This mechanism is similar to other materials, albeit in different range of wetting angles. We also identified other factors, such as composition and different adhesion of the FBS layers on H- and O-diamond, that can contribute to the cell array formation.

Electronic effects on the diamond-protein-cell interface were characterized by the SG-FET transistors based on the surface conductivity of nanocrystalline diamond where the gate was insulated solely by hydrogen surface atoms. We show that these transistors are fully operational and can serve as transducers (and partly also as amplifiers) of biological and/or environmental characteristics to electrical signals. Adsorption of proteins from the FBS-enriched cultivation medium and subsequent cultivation of cells on it led to a shift in transfer characteristics of the transistor in the range of 40–130 mV. This shift is the result of the adsorption of a thin film of proteins onto the diamond surface as confirmed by AFM. These shifts cannot be due to electrostatic field effect because it acts in the opposite direction. We proposed a model in which the proteins replace the ions in the very vicinity of the diamond surface. The negative shift in the transfer characteristics then arises from the lower conductivity of diamond itself, in agreement with the lowered transconductance. Related changes in the SG-FET gate currents

suggest that the FBS layer can block and under certain conditions also promote the transfer of charge across the interface between diamond and the solution.

The above findings and conclusions are significant for prospective application of the unique properties of diamond in bio-sensors, bio-electronics as well as other fields. At the same time we showed that the diamond represents an ideal substrate for studies of molecules in general as it can provide atomically flat and hard surface with well defined and widely adjustable wetting, chemical, and electronic properties.

9. Acknowledgements

I gratefully acknowledge and appreciate long-term continuous support from my students and colleagues in our research team, in our department of Thin Films and Nanostructures, other groups in the Institute of Physics as well as from our numerous collaborators in the Czech Republic and abroad. Without their hard work, ideas, advices and other contributions the presented results could hardly become reality. I also express my deep gratitude to my wife, my parents and other family members for their support, understanding as well as patience with sometimes very long working days and stressed moods.

The presented research work could not be done also without the substantial financial support by national grant projects such as KAN400100701 (Nanotechnology for Society, ASCR), P108/12/G108 (GACR Center of Excellence), P108/12/0996 (GACR), LM2011026 (MŠMT), LC510 (MŠMT), LC06040 (MŠMT), IAAX00100902 (GAAV), 202/09/H041 (GACR support for doctoral students), institutional Research Plan AV0Z10100521, and Fellowship J.E. Purkyně (ASCR).

10. Abstract

In this habilitation thesis we present the influence of micro-structured morphology and atomic termination of diamond surfaces on cell growth and assembly. We investigate the influence of key parameters such as seeding concentration of cells, type of the applied cells and concentration of fetal bovine serum (FBS) in the cultivation medium. We show that the adsorption of proteins from the FBS serum is the fundamental factor. Atomic force microscopy (AFM) both in solution and in air is applied to characterize properties of the FBS layers adsorbed on differently terminated diamond substrates. In order to recognize physisorption or chemisorption of organic molecules to diamond we develop and employ novel methodology that is based on the combination of advanced AFM and Kelvin force microscopy (KFM) or scanning electron microscopy (SEM). We demonstrate its use on the protein-diamond interface as well as on DNA-diamond interface and PPy-diamond heterojunction. The influence of proteins and cells on the electronic properties of diamond is characterized by employing a field-effect transistor based on hydrogen-terminated diamond, gate of which is exposed to a solution (SG-FET). Role of grain boundaries in nanocrystalline diamond is resolved and shown not to be detrimental for its function. At the same time we show that the diamond represents an ideal substrate for studies of molecules in general.

11. References

[1] J. Shakenraad, H. Busscher, *Cell-polymer interactions:the influence of protein adsorption*, Colloid Surf. 42 (1989) 331.

[2] G. Zhao, O. Zinger, Z. Schwartz, M. Wieland, D. Landolt, B. D. Boyan, *Osteoblast-like cells are sensitive to submicron-scale surface structure*, Clin. Oral. Implant. Res. 17 (2006) 258.

[3] A. Kromka, B. Rezek, M. Kalbacova, V. Baresova, J. Zemek, C. Konak, M. Vanecek, *Diamond seeding and growth of hierarchically structured films for tissue engineering*, Adv. Eng. Mater. 11 (2009) B71.

[4] M. Kalbacova, B. Rezek, V. Baresova, C. Wolf-Brandstetter, A. Kromka, *Nano-scale topography of nanocrystalline diamonds promotes differentiation of osteoblasts*, Acta Biomaterialia 5 (2009) 3076.

[5] O. Babchenko, A. Kromka, K. Hruska, M. Kalbacova, A. Broz, M. Vanecek, *Fabrication of nano-structured diamond films for SAOS-2 cell cultivation*, phys. stat. sol. (b) 206 (2009) 2033.

[6] M. Tanaka, A. Takayama, E. Ito, H. Sunami, S. Yamamoto, M. Shimomura, *Effect of pore size of self-organized honeycomb-patterned polymer films on spreading, focal adhesion, proliferation, and function of endothelial cells*, J. Nanosci. Nanotechnol. 7 (2007) 763.

[7] M. M. Browne, G. V. Lubarsky, M. R. Davidson, R. H. Bradley, *Protein adsorption onto polystyrene surfaces studied by XPS and AFM*, Surf. Sci. 553 (2004) 155.

[8] B. Rezek, E. Ukraintsev, L. Michalíková, A. Kromka, J. Zemek, M. Kalbacova, *Adsorption of fetal bovine serum on H/O-terminated diamond studied by atomic force microscopy*, Diam. Relat. Mater. 18 (2009) 918.

[9] M. Kalbacova, M. Kalbac, L. Dunsch, A. Kromka, M. Vanecek, B. Rezek, U. Hempel, S. Kmoch, *The effect of SWCNT and nano-diamond films on human osteoblast cells*, phys. stat. sol. (b) 244 (11) (2007) 4356.

[10] L. Grausova, L. Bacakova, A. Kromka, M. Vanecek, B. Rezek, V. Lisa, *Molecular markers of adhesion, maturation and immune activation of human osteoblast-like MG63 cells on nanocrystalline diamond films*, Diam. Relat. Mater. 18 (2009) 258.

[11] C. E. Nebel, D. Shin, B. Rezek, N. Tokuda, H. Uetsuka, H. Watanabe, *Diamond and biology*, J. R. Soc. Interface 4 (2007) 439.

[12] S. Potocky, A. Kromka, J. Potmesil, Z. Vorlicek, M. Vanecek, M. Michalka, *Investigation of nanocrystalline diamond films grown on silicon and glass at substrate temperature below 400°C*, Diamond Relat. Mater. 16 (2007) 744–747.

[13] A. Kromka, B. Rezek, Z. Remeš, M. Michalka, M. Ledinský, J. Zemek, J. Potměšil, M. Vaněček, *Formation of continuous nanocrystalline diamond layer on glass and silicon at low temperatures*, Chem. Vap. Deposition 14 (2008) 181.

[14] K. Tsugawa, M. Ishihara, J. Kim, Y. Koga, M. Hasegawa, *Nanocrystalline diamond film growth on plastic substrates at temperatures below 100°C from low-temperature plasma*, Phys. Rev. B 82 (2010) 125460.

[15] A. Kromka, O. Babchenko, T. Izak, K. Hruska, B. Rezek, *Linear antenna microwave plasma CVD deposition of diamond films over large areas*, Vacuum 86 (2012) 776.

[16] H. Kozak, A. Kromka, O. Babchenko, B. Rezek, *Directly grown nanocrystalline diamond field-effect transistor microstructures*, Sensor Lett. 8 (2010) 482.

[17] P. Hubík, J. Mareš, H. Kozak, A. Kromka, B. Rezek, J. Krištofík, D. Kindl, *Linear antenna microwave plasma CVD deposition of diamond films over large areas*, Diam. Relat. Mater. 24 (2012) 63.

[18] M. Krátká, A. Kromka, E. Ukraintsev, A. Brož, M. Kalbacova, B. Rezek, *Function of thin film nanocrystalline diamond-protein SGFET independent of grain size*, Sens. Actuators B 20 (2012) 239.

[19] L. Tang, C. Tsai, W. Gerberich, L. Kruckeberg, D. Kania, *Biocompatibility of chemical-vapour-deposited diamond*, Biomaterials 16 (6) (1995) 483–488.

[20] P. Bajaj, D. Akin, A. Gupta, D. Sherman, B. Shi, O. Auciello, R. Bashir, *Ultrananocrystalline diamond film as an optimal cell interface for biomedical applications*, Biomed. Devices 9 (2007) 787.

[21] S. G. Ri, T. Mizumasa, Y. Akiba, Y. Hirose, T. Kurosu, M. Iida, *Formation mechanism of p-type surface conductive layer on deposited diamond films*, Jpn. J. Appl. Phys. 34 (1995) 5550.

[22] B. Rezek, C. Sauerer, C. E. Nebel, M. Stutzmann, J. Ristein, L. Ley, E. Snidero, P. Bergonzo, *Fermi level on hydrogen terminated diamond surfaces*, Appl. Phys. Lett. 82 (2003) 2266.

[23] V. Chakrapani, J. C. Angus, A. B. Anderson, S. D. Wolter, B. R. Stoner, G. U. Sumanasekera, *Charge transfer equilibria between diamond and an aqueous oxygen electrochemical redox couple*, Science 318 (2007) 1424.

[24] W. Yang, O. Auciello, J. E. Butler, W. Cai, J. A. Carlisle, J. E. Gerbi, D. M. Gruen, T. Knickerbocker, T. L. Lasseter, J. J. N. Russel, L. M. Smith, R. J. Hamers, *DNA-modified nanocrystalline diamond thin films as stable, biologically active substrates*, Nature Mat. 1 (2002) 253.

[25] A. Härtl, E. Schmich, J. A. Garrido, J. Hernando, S. C. R. Catharino, S. Walter, P. Feulner, A. Kromka, D. Steinmüller, M. Stutzmann, *Protein-modified nanocrystalline diamond thin films for biosensor applications*, Nature Mat. 3 (2004) 736.

[26] P. Strobel, M. Riedel, J. Ristein, L. Ley, *Surface transfer doping of diamond*, Nature 430 (2004) 439.

[27] B. Rezek, D. Shin, H. Uetsuka, C. E. Nebel, *Microscopic diagnostics of DNA molecules on mono-crystalline diamond*, phys. stat. sol. (a) 204 (2007) 2888.

[28] P. Ang, K. Loh, T. Wohland, M. Nesladek, E. V. Hove, *Supported lipid bilayer on nanocrystalline diamond: dual optical and field-effect sensor for membrane disruption*, Adv. Funct. Mater. 9 (2009) 109.

[29] B. Rezek, H. Kozak, A. Kromka, *Stabilizing diamond surface conductivity by phenol-formaldehyde and acrylate resins*, Thin Solid Films 517 (2009) 3738.

[30] W. Gajewski, M. Huth, F. Buth, B. Nickel, M. Stutzmann, J. A. Garrido, *Photoresponse and morphology of pentacene thin films modified by oxidized and reduced diamond surfaces*, Phys. Rev. B 80 (2009) 235311.

[31] M. Kalbacova, L. Michalíková, V. Barešová, A. Kromka, B. Rezek, S. Kmoch, *Adhesion of osteoblasts on chemically patterned nanocrystalline diamonds*, phys. stat. sol. (b) 245 (2008) 2124.

[32] L. Michalíková, B. Rezek, A. Kromka, M. Kalbacova, *CVD diamond films with hydrophilic micro-patterns for self-organisation of human osteoblasts*, Vacuum 84 (2009)

61.
[33] B. Rezek, L. Michalíková, E. Ukraintsev, A. Kromka, M. Kalbacova, *Micro-pattern guided adhesion of osteoblasts on diamond surfaces*, Sensors 9 (2009) 3549.
[34] D. Shin, B. Rezek, N. Tokuda, D. Takeuchi, H. Watanabe, T. Nakamura, T. Yamamoto, C. E. Nebel, *Photo- and electrochemical bonding of DNA to single crystalline CVD diamond*, phys. stat. sol. (a) 203 (2006) 3245.
[35] B. Rezek, J. Čermák, A. Kromka, M. Ledinský, J. Kočka, *Photovoltage effects in polypyrrole-diamond nanosystem*, Diamond Relat. Mater. 18 (2009) 249.
[36] H. Kawarada, *Hydrogen-terminated diamond surfaces and interfaces*, Surf. Sci. Rep. 26 (7) (1996) 205.
[37] F. Maier, J. Ristein, L. Ley, *Electron affinity of plasma-hydrogenated and chemically oxidized diamond (100) surfaces*, Phys. Rev. B 64 (2001) 65411.
[38] C. E. Nebel, B. Rezek, D. Shin, H. Watanabe, T. Yamamoto, *Electronic properties of H-terminated diamond in electrolyte solutions*, J. Appl. Phys. 99 (2006) 033711.
[39] B. Rezek, D. Shin, H. Watanabe, C. E. Nebel, *Intrinsic hydrogen-terminated diamond as ion-sensitive field effect transistor*, Sens. Actuators B 122 (2007) 596.
[40] M. Dankerl, A. Reitinger, M. Stutzmann, J. A. Garrido, *Resolving the controversy on the pH sensitivity of diamond surfaces*, phys. stat. sol. RRL 2 (2007) 31.
[41] B. Rezek, M. Krátká, A. Kromka, M. Kalbacova, *Effects of protein inter-layers on cell-diamond FET characteristics*, Biosens. Bioelectron. 26 (2010) 1307.
[42] M. Dankerl, S. Eick, B. Hofmann, M. Hauf, S. Ingebrandt, A. Offenhäusser, M. Stutzmann, J. A. Garrido, *Diamond transistor array for extracellular recording from electrogenic cells*, Adv. Funct. Mater. 19 (2009) 2915.
[43] H. Kozak, A. Kromka, M. Ledinský, B. Rezek, *Enhancing nanocrystalline diamond surface conductivity by deposition temperature and chemical post-processing*, phys. stat. sol. (a) 206 (2009) 276.
[44] M. Kalbacova, S. Roessler, U. Hempel, R. Tsaryk, K. Peters, D. Scharnweber, C. Kirkpatrick, P. Dieter, *The effect of electrochemically simulated titanium cathodic corrosion products on ROS production and metabolic activity of osteoblasts and monocytes/macrophages*, Biomaterials 28 (2007) 3263.
[45] B. Rezek, D. Shin, T. Nakamura, C. E. Nebel, *Geometric properties of covalently bonded DNA on single-crystalline diamond*, J. Am. Chem. Soc. 128 (2006) 3884.
[46] C. Popov, W. Kulisch, J. Reithmaier, T. Dostalova, M. Jelinek, N. Anspach, C. Hammann, *Bioproperties of nanocrystalline diamond/amorphous carbon composite films*, Diamond Relat. Mater. 16 (2007) 735.
[47] E. Ukraintsev, B. Rezek, A. Kromka, A. Broz, M. Kalbacova, *Long-term adsorption of fetal bovine serum on H/O-terminated diamond studied in-situ by atomic force microscopy*, phys. stat. sol. (b) 246 (2009) 2832.
[48] B. Rezek, E. Ukraintsev, A. Kromka, M. Ledinský, A. Brož, L. Nosková, H. Hartmannová, M. Kalbacova, *Assembly of osteoblastic cell micro-arrays on diamond guided by protein pre-adsorption*, Diam. Relat. Mater. 19 (2010) 153.
[49] B. Rezek, J. Čermák, A. Kromka, M. Ledinský, P. Hubík, V. Cimrová, A. Fejfar, *Synthesis, structure, and opto-electronic properties of organic-based nanoscale heterojunctions*, Nanoscale Res. Lett. 6 (2011) 238.

[50] E. Ukraintsev, A. Kromka, W. Janssen, K. Haenen, B. Rezek, *Controlling physical and chemical bonding of polypyrrole to boron doped diamond by surface termination*, Int. J. Electrochem. Sci. 8 (2013) 17.

[51] B. Rezek, D. Shin, C. E. Nebel, *Properties of hybridized DNA arrays on single-crystalline undoped and boron-doped (100) diamonds studied by atomic force microscopy in electrolytes*, Langmuir 23 (2007) 7626.

[52] S. Stehlik, T. Petit, H. A. Girard, J.-C. Arnault, A. Kromka, B. Rezek, *Nanoparticles assume electrical potential according to substrate, size and surface termination*, Langmuir 29 (2013) 17.

[53] S. Sadewasser, T. Glatzel (Eds.), Kelvin probe force microscopy, Springer-Verlag Berlin, Heidelberg, 2012.

[54] C. Agnes, S. Ruffinatto, E. Delbarre, A. Roget, J.-C. Arnault, F. Omnes, P. Mailley, *New one step functionalization of polycrystalline diamond films using amine derivatives*, Mater. Sci. Eng. 16 (2010) 012001.

[55] J. Čermák, B. Rezek, A. Kromka, M. Ledinský, J. Kočka, *Electrochemical synthesis and electronic properties of polypyrrole on intrinsic diamond*, Diamond Relat. Mater. 18 (2009) 1098.

[56] W. Kaminski, V. Rozsíval, P. Jelínek, *Theoretical study of electronic and transport properties of PPy–Pt(111) and PPy–C(111):H interfaces*, J. Phys.: Condens. Matter 22 (2010) 045003.

[57] B. Rezek, C. E. Nebel, *Electronic properties of plasma hydrogenated diamond surfaces: a microscopic study*, Diamond Relat. Mater. 15 (2006) 1374.

[58] B. Rezek, C. E. Nebel, *Kelvin force microscopy on diamond surfaces and devices*, Diamond Relat. Mater. 14 (2005) 466.

[59] H. Kawarada, A. R. Ruslinda, *Diamond electrolyte solution gate FETs for DNA and protein sensors using DNA/RNA aptamers*, phys. stat. sol. (a) 208 (2011) 2005.

[60] T. Sakata, I. Makino, S. Kita, *Real-time and noninvasive monitoring of sea urchin embryo activity using semiconductor devices*, Eur. Biophys. J. 40 (2011) 699.

[61] M. Krátká, A. Kromka, A. Brož, M. Kalbáčová, B. Rezek, *Characteristics of nanocrystalline diamond SGFETs under cell culture conditions*, in: WDS'11 Proceedings of Contributed Papers, Part III, Matfyzpress, 2011, p. 160.

[62] J. L. R. Fernandez, B. Geiger, D. Salomon, A. Ben-Ze'v, *Overexpression of vinculin suppresses cell motility in BALB/c 3T3 cells*, Cell. Motil. Cytoskeleton 22 (1992) 127.

[63] F. Maier, M. Riedel, B. Mantel, J. Ristein, L. Ley, *Origin of surface conductivity in diamond*, Phys. Rev. Lett. 85 (2000) 3472.